JOURNAL OF COMPUTATIONAL PHYSICS **132,** 276–284 (1997)
ARTICLE NO. CP965620

Fast Algorithms for Triangular Josephson Junction Arrays

Sujay Datta and Deshdeep Sahdev

Department of Physics, Indian Institute of Technology, Kanpur, 208 016, India
E-mail: ds@iitk.ernet.in

Received April 18, 1996; revised September 25, 1996

We develop fast algorithms for the numerical study of two-dimensional triangular Josephson junction arrays. The Dirac bra-ket formalism is introduced in the context of such arrays. We note that triangular arrays can have both hexagonal and rectangular periodicity and develop algorithms for each. Boundaries are next introduced and fast algorithms for finite arrays are developed. © 1997 Academic Press

1. INTRODUCTION

Josephson junction arrays (JJAs) have recently evoked wide interest among theorists and experimentalists alike [1]. This is in part because they can now be routinely fabricated with controlled variation of junction parameters in various sizes and shapes [2]. From the theoretical standpoint, they are physical realisations of the widely studied 2D XY Model [3]. Furthermore, they exhibit a range of interesting phenomena when subjected to magnetic fields and current drives. These phenomena are the foci of several experimental [4] and numerical studies [5–8]. The studies indicate that vortices, which are natural excitations of the system, play an important role in determining both the equilibrium and dynamical properties of these arrays. The behaviour of vortices, in turn, depends in large part on the vortex pinning potential, which arises from the discreteness of the lattice. Many features of vortex behaviour are thus better understood by varying the pinning potential. This can be achieved by switching to a triangular lattice, which has a ~5 times smaller pinning potential than a square array [9]. Triangular lattices are hence better suited for the study of the dynamics of an ideal 2D gas of vortices [10]. They also provide a better chance for the observation of ballistic vortex motion, i.e., the motion of a ''massive'' vortex through a force-free region due to its own inertia, which has been predicted theoretically [11–14] and has to some extent been investigated experimentally [15] and numerically [16–20]. The geometry of the hexagon, which occurs naturally in triangular arrays, allows us to conveniently study the Aharanov–Casher effect wherein vortices, as quantum objects, can interfere constructively or destructively after following two different paths enclosing a charge placed at the center of the hexagon [21]. The ground state configuration of triangular arrays under the application of an external magnetic field has unique features of its own. For example, domain wall superlattices [22] occur at characteristic values of f, the quantum of magnetic flux threading a plaquette, and there is an accidental degeneracy of the ground state [23] for $f = \frac{1}{3}$ and $\frac{1}{4}$. In fact, there are indications that the case of $f = \frac{1}{4}$ belongs to the same universality class as the fully frustrated $f = \frac{1}{2}$ case of the square lattice [24, 25]. It has also been observed that the presence or absence of fractional Shapiro steps depends on the relative orientation of the lattice and the external current drive [26]. Lastly, we note that a triangular configuration of three capacitive [27] and resistive [28] junctions offers the simplest geometry capable of sustaining a vortex while being amenable to explicit theoretical analysis.

With the size of experimental arrays increasing constantly and with the number of interesting effects best seen in large arrays going up as well, there is a growing need to find methods to enhance the computational efficiency of the algorithms used to numerically simulate such arrays. These algorithms must address the problem of integrating the set of coupled non-linear first-order differential equations, which results from the application of total current conservation (TCC) [29] to each superconducting island of the array. The issues involved are best explained in the context of overdamped junctions. We recall that the total current passing through such junctions can be broken up into two ''channels'' namely, superconductive and resistive. Using the RSJ model [30], one can then write the evolution equations for such an array as

$$\sum_{\langle ij \rangle} \frac{\hbar}{2eR} \frac{d\theta_{ij}}{dt} + I_c \sin \theta_{ij} = I_i^{ext} \qquad \forall i, \tag{1}$$

where $\theta_{ij} = \theta_i - \theta_j$, I_c is the single junction critical current, R is the shunt resistance, I^{ext} the external current, and the

0021-9991/97 $25.00

$\langle ij \rangle$ are the nearest neighbours of i. For an $N_x \times N_y \equiv N$ array, this set of differential equations can be written in matrix notation as

$$G_0^{-1}[\dot{\theta}] = [d], \tag{2}$$

where the time differentiation is with respect to $\tau = t(2eI_cR)/\hbar$ and $[d]$ and $[\dot{\theta}]$ are the super-current divergence (inclusive of I^{ext} wherever present) and the voltage vectors, respectively. Using the gauge-fixing condition, $\sum_i \dot{\theta}_i = 0$ one can invert this relation to get

$$[\dot{\theta}] = \tilde{G}[d]. \tag{3}$$

Each integration time step thus requires the multiplication of an $N \times N$ array $\tilde{G}$ with an $N \times 1$ vector $[d]$. The complexity of the procedure as it stands is therefore $\mathcal{O}(N^2)$. Eikmans and Himbergen [31] devised a method for reducing the complexity to $\mathcal{O}(N \ln N)$ for square arrays. Dominguez *et al.* [8] combined the Fourier and the cyclic reduction method to further increase the efficiency. Datta *et al.* [32] introduced a fast algorithm for arrays with missing bonds and extended the scope of such procedures to the case of bus-bars through which a current could be injected or extracted. No fast algorithms have however been discussed so far in the literature for the case of triangular arrays, although one such algorithm has, reportedly, been used by Dominguez *et al.* [33]. It is the purpose of this work to fill this lacuna.

The paper is organized as follows. In Section 2 we discuss the notation followed consistently through the entire manuscript. The fast algorithms for the periodic triangular lattices are developed in Section 3 while Section 4 extends them to finite arrays as well. We summarise our conclusions and discuss various points in Section 5.

2. NOTATION

The algorithms which we develop in this paper can very conveniently be discussed in terms of the bra-ket formalism of Dirac [34, 35]. A given state of the system corresponds to a specific configuration of the θ's and can be denoted by $|\theta\rangle$. In the position basis $\{|\mathbf{x}\rangle \equiv |x_1, x_2\rangle\}$, the components of $|\theta\rangle$ are obtained by taking the usual projections $\langle x_1, x_2|\theta\rangle = \theta(x_1, x_2)$. We note that the coordinates (x_1, x_2) of the various lattice sites are related to the labels i used in Eq. (2) by $(x - x_0) + (y - y_0)N_x + 1$ where the (x_0, y_0) are the coordinates at the bottom-left corner of the array. We could alternatively consider the components $\theta(k_1, k_2) = \langle \mathbf{k}|\theta\rangle$ in the momentum basis $\{|\mathbf{k}\rangle\}$. These are related to $\theta(x_1, x_2)$ by the unitary transformation matrix $\langle \mathbf{k}|\mathbf{x}\rangle$,

$$\theta(k_1, k_2) = \sum_{\mathbf{x}} \langle \mathbf{k}|\mathbf{x}\rangle\langle \mathbf{x}|\theta\rangle, \tag{4}$$

where the summation is to be carried out over all the lattice points. The validity of this equation as also the unitarity of $\langle \mathbf{k}|\mathbf{x}\rangle$ rests on the completeness of the two bases in the N-dimensional space of interest,

$$I = \sum_{\mathbf{x}} |\mathbf{x}\rangle\langle \mathbf{x}| = \sum_{\mathbf{k}} |\mathbf{k}\rangle\langle \mathbf{k}|, \tag{5}$$

where I is the N dimensional identity matrix. Both bases are further assumed to be orthonormal, i.e.,

$$\langle \mathbf{x}|\mathbf{x}'\rangle = \delta_{x_1,x_1'}\delta_{x_2,x_2'} \quad \text{and} \quad \langle \mathbf{k}|\mathbf{k}'\rangle = \delta_{k_1,k_1'}\delta_{k_2,k_2'}. \tag{6}$$

We note that the delta functions occurring in Eq. (6) are the kronecker (as opposed to dirac) deltas. Furthermore, Eq. (6) indicates that in the position basis, the vector $|\mathbf{x}\rangle$ is zero at all points other than $\mathbf{x} \equiv (x_1, x_2)$ where it is 1.

The $\dot{\theta}_i$ and the divergence d_i similarly give rise to the vectors $|\dot{\theta}\rangle$ and $|d\rangle$. Equation (3) is then

$$G_0^{-1}|\dot{\theta}\rangle = |d\rangle \tag{7}$$

written out in the position basis.

The underpinnings of the fast algorithms can now be made transparent by writing Eq. (3) as

$$\begin{aligned}\langle \mathbf{x}|\dot{\theta}\rangle &= \langle \mathbf{x}|\tilde{G}|d\rangle \\ &= \sum_{\mathbf{x}'}\sum_{\mathbf{k}}\sum_{\mathbf{k}'} \langle \mathbf{x}|\mathbf{k}\rangle\langle \mathbf{k}|\tilde{G}|\mathbf{k}'\rangle\langle \mathbf{k}'|\mathbf{x}'\rangle\langle \mathbf{x}'|d\rangle.\end{aligned} \tag{8}$$

We note that the r. h. s. of Eq. (8) involves

(i) Evaluating $\sum_{\mathbf{x}'} \langle \mathbf{k}'|\mathbf{x}'\rangle\langle \mathbf{x}'|d\rangle = \langle \mathbf{k}'|d\rangle$. This is the forward transform W and can be executed in certain cases with complexity $\mathcal{O}(N \ln N)$.

(ii) Multiplying $\langle \mathbf{k}'|d\rangle$ by $\langle \mathbf{k}|\tilde{G}|\mathbf{k}'\rangle$, i.e., the operator $\tilde{G}$ expressed in the $\mathbf{k}$ basis, to get $\langle \mathbf{k}|d'\rangle$. If $\tilde{G}$ happens to be diagonal in this basis, the multiplication can be carried out in N steps.

(iii) Taking the backward transform $\tilde{W}$, i.e., $\sum_{\mathbf{k}} \langle \mathbf{x}|\mathbf{k}\rangle\langle \mathbf{k}|d'\rangle$. Here too, the complexity, for some cases, is $\mathcal{O}(N \ln N)$.

It follows that we have a fast algorithm for a given lattice as soon as we have discovered a basis $\{|\mathbf{k}\rangle\}$ which (i) is related to the position basis $\{|\mathbf{x}\rangle\}$ by a fast transform of some sort and (ii) completely or almost completely diagonalizes the corresponding $\tilde{G}$ or G_0^{-1}.

For a periodic $L_1 \times L_2$ square lattice (where L_1 and

L_2 refer to the lengths in the x and y directions, respectively)

$$\langle \mathbf{x}'|G_0^{-1}|\mathbf{x}\rangle = (4\delta_{\mathbf{x},\mathbf{x}'} - \delta_{\mathbf{x},\mathbf{x}'+\hat{e}_1} - \delta_{\mathbf{x},\mathbf{x}'-\hat{e}_1} - \delta_{\mathbf{x},\mathbf{x}'+\hat{e}_2} - \delta_{\mathbf{x},\mathbf{x}'-\hat{e}_2}) \tag{9}$$

and the basis defined by

$$\langle \mathbf{x}|\mathbf{k}\rangle = \frac{1}{\sqrt{L_1 L_2}} \exp(i\mathbf{k}\cdot\mathbf{x}) \tag{10}$$

with $k_i = 2n_i\pi/L_i$, does the job. The transforms W and $\tilde{W}$ in this case are the usual direct and inverse fast fourier transforms, respectively, and $\tilde{G}$ is clearly diagonal:

$$\begin{aligned}\langle \mathbf{k}'|\tilde{G}|\mathbf{k}\rangle &= \frac{1}{4 - 2\cos k_x - 2\cos k_y}\langle \mathbf{k}'|\mathbf{k}\rangle \\ &= \frac{1}{\lambda_{k_x,k_y}}\delta_{\mathbf{k}',\mathbf{k}}.\end{aligned} \tag{11}$$

For a finite square lattice, the G_0^{-1} matrix, on the other hand, is

$$\begin{aligned}\langle \mathbf{x}'|G_0^{-1}|\mathbf{x}\rangle = {} & (\delta_{\mathbf{x},\mathbf{x}'} - \delta_{\mathbf{x},\mathbf{x}'-\hat{e}_1})(1 - \delta_{x_1,x_0}) \\ & + (\delta_{\mathbf{x},\mathbf{x}'} - \delta_{\mathbf{x},\mathbf{x}'+\hat{e}_1})(1 - \delta_{x_1,x_0+L_1-1}) \\ & + (\delta_{\mathbf{x},\mathbf{x}'} - \delta_{\mathbf{x},\mathbf{x}'-\hat{e}_2})(1 - \delta_{x_2,y_0}) \\ & + (\delta_{\mathbf{x},\mathbf{x}'} - \delta_{\mathbf{x},\mathbf{x}'+\hat{e}_2})(1 - \delta_{x_2,y_0+L_2-1})\end{aligned} \tag{12}$$

where the (x_0, y_0) are the coordinates of the bottom-left edge of the array. The $\mathbf{k}$-basis is now given by

$$\langle \mathbf{x}|\mathbf{k}\rangle = N_{\mathbf{k}} \cos k_1 x_1 \cos k_2 x_2, \tag{13}$$

where $k_i = n\pi/L_i$, $\frac{1}{2} \le x_i \le L_i + \frac{1}{2}$; $i = 1, 2$ and $N_{\mathbf{k}}$ are the normalisation constants. We note that the set of $|\mathbf{k}\rangle$ vectors spans the vector space of states/configurations and moreover diagonalizes $\tilde{G}$. The transforms W and $\tilde{W}$ are now the direct and inverse fast discrete cosine transforms.

The perceptive reader would have noticed that the $\{|\mathbf{k}\rangle\}$ basis is different for different lattices. Strictly speaking, we should introduce a new symbol each time to indicate this. However, that would make the notation cumbersome. We, accordingly, use the symbol $\{|\mathbf{k}\rangle\}$ uniformly and let the context and the explicitly stated form of $\langle \mathbf{x}|\mathbf{k}\rangle$ decide its precise meaning.

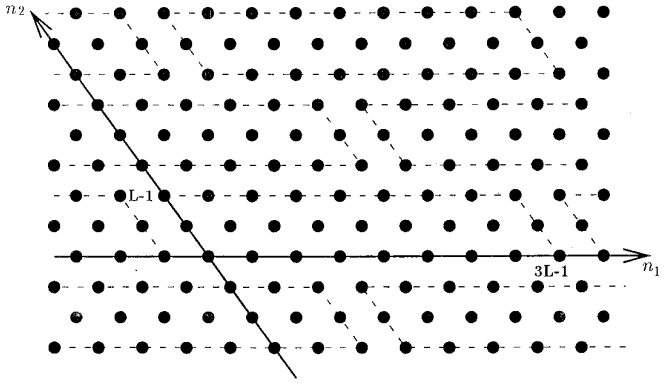

FIG. 1. A hexagonally periodic tiling, with $L_1 = L_2 = L = 3$, of an infinite triangular lattice.

3. FAST ALGORITHMS FOR PERIODIC TRIANGULAR LATTICES

In contrast to a square array, a triangular lattice can have hexagonal as well as rectangular periodicity. We recall that all variables $\eta(x_1, x_2)$ defined on a $L_1 \times L_2$ rectangularly periodic array must satisfy

$$\eta(x_1, x_2) = \eta(x_1 + L_1, x_2) = \eta(x_1, x_2 + L_2). \tag{14}$$

The analogous conditions for a hexagonally periodic triangular lattice are

$$\begin{aligned}\eta(x_1, x_2) &= \eta(x_1 + 2L_1 + L_2, x_2) \\ &= \eta(x_1 + L_1 + L_2, x_2 + L_2) \\ &= \eta(x_1 + L_1, x_2 + 2L_2).\end{aligned} \tag{15}$$

We note that conditions (15) make sense only for lattices containing $L_2(2L_1 + L_2)$ points. Furthermore, when imposed on an infinite triangular lattice, these conditions produce a tiling (see Fig. 1) of the latter by the array in question (this has been referred to as the ''fundamental period'' in Ref. [36]). This tiling is quite distinct from the one which follows from the conditions (14). If corresponding points on different tiles are now identified with one another, one immediately obtains the connectivity of points on the boundary of each tile. For example, in the rectangularly periodic lattice of Fig. 2, the points carrying the same labels on the top and bottom rows (left and right columns) are treated as identical. In other words, the lattice is folded like a torus. The folding of the hexagonally periodic lattice of Fig. 3, on the other hand, is quite unfamiliar but follows straightforwardly from the tiling displayed in

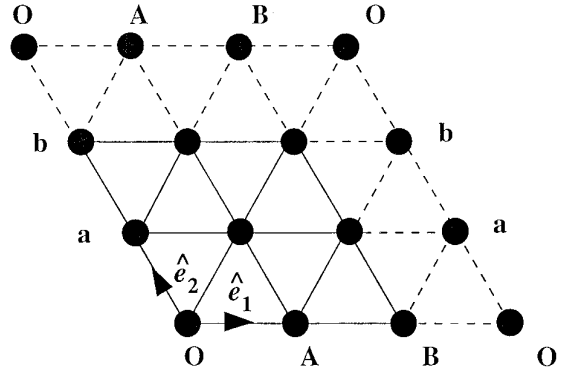

FIG. 2. A rectangularly periodic triangular lattice with $L_1 = L_2 = 3$. $\hat{e}_1$ and $\hat{e}_2$ are unit vectors. The points O, A, B, C, a, and b are to be identified.

Fig. 3. The points to be identified here have, as before, been given identical labels. We should mention that the above identification can be physically realised through electrical shorts. For further details on hexagonal periodicity, we refer the reader to Ref. [36]. Apart from specifying the connectivity of an arbitrary site, the underlying periodicity limits the choice of eigenfunctions $\langle \mathbf{x}|\mathbf{k}\rangle$ needed to diagonalize the corresponding laplacian G_0^{-1}. We discuss this choice for each type of periodicity in turn.

3.1. *The Rectangularly Periodic Case*

A convenient choice of coordinate system for a rectangularly periodic triangular array is shown in Fig. 2. The eigenfunctions in this case can be taken to be $\propto \exp(i\mathbf{k}\cdot\mathbf{x})$ where $\mathbf{k} = k_1\hat{e}_1 + k_2\hat{e}_2$ and $\mathbf{r} = x_1\hat{e}_1 + x_2\hat{e}_2$ with $\hat{e}_1\cdot\hat{e}_2 = -\frac{1}{2}$. The action of G_0^{-1} on these eigenfunctions is best described in terms of $\kappa_1 = k_1 + k_2/2$ and $\kappa_2 = k_2 + k_1/2$. Indeed,

$$\langle \mathbf{x}|G_0^{-1}|\mathbf{x}'\rangle = (6\delta_{\mathbf{x},\mathbf{x}'} - \delta_{\mathbf{x},\mathbf{x}'\pm\hat{e}_1} - \delta_{\mathbf{x},\mathbf{x}'\pm\hat{e}_2} - \delta_{\mathbf{x},\mathbf{x}'\pm(\hat{e}_2-\hat{e}_2)}) \quad (16)$$

whence

$$\begin{aligned}\langle \mathbf{x}|G_0^{-1}|\mathbf{k}\rangle &= \sum_{\mathbf{x}'}\langle \mathbf{x}|G_0^{-1}|\mathbf{x}'\rangle\langle \mathbf{x}'|\mathbf{k}\rangle \\ &= \sum_{\mathbf{x}'}\langle \mathbf{x}|G_0^{-1}|\mathbf{x}'\rangle \exp i\mathbf{k}\cdot\mathbf{x}' \\ &= [6 - 2\cos\kappa_1 - 2\cos\kappa_2 - 2\cos(\kappa_1-\kappa_2)] \\ &\quad \exp i(\kappa_1 x_1 + \kappa_2 x_2) \\ &= \lambda_{\kappa_1,\kappa_2}\langle \mathbf{x}|\mathbf{k}\rangle.\end{aligned} \quad (17)$$

It is noteworthy that $\lambda_{\kappa_1,\kappa_2}$ has all the 12 symmetries of the hexagonal group:

$$\begin{aligned}\lambda_{\kappa_1,\kappa_2} &= \lambda_{-\kappa_1,-\kappa_2} = \lambda_{\pm\kappa_1,\pm(\kappa_1-\kappa_2)} = \lambda_{\mp(\kappa_1-\kappa_2),\pm\kappa_2} \\ &= \lambda_{\mp\kappa_2,\pm(\kappa_1-\kappa_2)} = \lambda_{\pm\kappa_2,\pm\kappa_1} = \lambda_{\pm(\kappa_1-\kappa_2),\pm\kappa_1}.\end{aligned} \quad (18)$$

Due to rectangular periodicity (Eq. (14)), the wavevectors have to satisfy the quantization conditions $\kappa_i = (2n_i\pi)/L_i$, $i = 1, 2$, with $n_i = 0, 1, \ldots, L_i - 1$ and the Green's function (see Jackson [37] for definition) for the rectangularly periodic triangular lattice reads, accordingly,

$$\tilde{G}(\mathbf{x},\mathbf{x}') = \frac{4}{L_1L_2}\sum_{\boldsymbol{\kappa}\neq 0}\frac{\exp i[\kappa_1(x_1-x_1') + \kappa_2(x_2-x_2')]}{6 - 2\cos\kappa_1 - 2\cos\kappa_2 - 2\cos(\kappa_1-\kappa_2)}. \quad (19)$$

This is the same as the Green's function of a periodic square lattice with only the eigenvalues changed. Thus a knowledge of the $\mathcal{O}(N\ln N)$ algorithm for the square case immediately provides a fast algorithm for this configuration, as well.

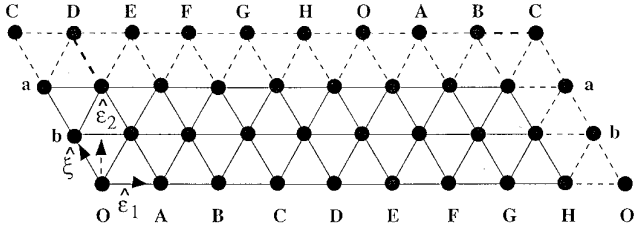

FIG. 3. A hexagonally periodic triangular lattice with $L_1 = L_2 = 3$ and consisting of $L_2(2L_1 + L_2)$ lattice points. The unit vectors, $\hat{\varepsilon}_1$, $\hat{\varepsilon}_2$, and $\hat{\xi}$, referred to in the text are as shown. Hexagonal periodicity results when the points O, A, B, C, D, E, F, G, H, a, and b are identified with one another.

3.2. *The Hexagonally Periodic Case*

The eigenfunctions of G_0^{-1} for this case can, once again, be written as $\exp(i\mathbf{k}\cdot\mathbf{x})$, provided we set $\mathbf{k} = k_1\hat{\varepsilon}_1 + k_2\hat{\varepsilon}_2$ and $\mathbf{x} = x_2\hat{\xi} + x_1\hat{\varepsilon}_1$ with $\hat{\varepsilon}_i\cdot\hat{\varepsilon}_j = \delta_{ij}$ and $\hat{\xi} = (\sqrt{3}/2)\hat{\varepsilon}_2 - (1/2)\hat{\varepsilon}_2$ (see Fig. 3). In terms of $\kappa_2 = (\sqrt{3}/2)k_2$, $\kappa_2 = (1/2)k_2$, these functions, on being normalized, take the form

$$\langle \mathbf{x}|\mathbf{k}\rangle = \frac{1}{\sqrt{L_2(2L_1+L_2)}}\exp i\{\kappa_1(2x_1 - x_2) + \kappa_2 x_2\}. \quad (20)$$

It is easily verified that the action of G_0^{-1} on $\langle \mathbf{x}|\mathbf{k}\rangle$ yields

$$
\begin{aligned}
&\langle \mathbf{x}|G_0^{-1}|\mathbf{k}\rangle \\
&= \sum_{\mathbf{x}'} \langle \mathbf{x}|G_0^{-1}|\mathbf{x}'\rangle\langle \mathbf{x}'|\mathbf{k}\rangle \\
&= N[6\delta_{x_1,x_1'}\delta_{x_2,x_2'} - \delta_{x_1\pm1,x_1'}\delta_{x_2,x_2'} - \delta_{x_1\pm1,x_1'}\delta_{x_2\pm1,x_2'} - \delta_{x_1,x_1'}\delta_{x_2\pm1,x_2'}] \\
&\quad \exp i\{\kappa_1(2x_1 - x_2) + \kappa_2 x_2)\} \\
&= N[6 - 2\cos(\kappa_1 + \kappa_2) - 2\cos(\kappa_1 - \kappa_2) - 2\cos(2\kappa_1)] \\
&\quad \exp i\{\kappa_1(2x_1 - x_2) + \kappa_2 x_2)\} \\
&= \lambda_{\kappa_1,\kappa_2} N \exp i\{\kappa_1(2x_1 - x_2) + \kappa_2 x_2)\}, \qquad (21)
\end{aligned}
$$

where $N = [L_2(2L_1 + L_2)]^{-1/2}$ is the appropriate normalization constant. The eigenvalues $\lambda_{\kappa_1,\kappa_2}$ are 12-fold degenerate and the corresponding eigenfunctions are easily checked to be

$$
\begin{aligned}
&\exp i\{\pm\kappa_1(2x_1 - x_2) + \kappa_2 x_2)\}, \\
&\exp i\{\pm\kappa_1(x_1 + x_2) + \kappa_2(x_1 - x_2)\}, \qquad (22) \\
&\exp i\{\pm\kappa_1(x_1 - 2x_2) + \kappa_2 x_2)\}
\end{aligned}
$$

and their complex conjugates.

All these wavefunctions can be made to respect the hexagonal periodicity of the lattice by simply quantizing κ_i. The quantized values of the momenta, for the case $L_1 = L_2 = L$, are

$$
\kappa_1 = (2n_1 - n_2)\frac{\pi}{3L} \qquad \text{and} \qquad \kappa_2 = \frac{n_2\pi}{L}, \qquad (23)
$$

where n_1 and n_2 are integers, $0 \le n_1 < 3L$, $0 \le n_2 < L$.

With this in hand, we can write the Green's function for the hexagonally periodic triangular lattice as

$$
\begin{aligned}
&\tilde{G}(x_1, x_2|x_1', x_2') \\
&= \frac{1}{3L^2} \sum_{n_1=0,n_2=0;(n_1,n_2)\neq 0}^{3L-1,L-1} \left(6 - 2\cos(2n_1 - n_2)\frac{2\pi}{3L}\right. \\
&\quad \left. - 2\cos(2n_2 - n_1)\frac{2\pi}{3L} - 2\cos(n_1 + n_2)\frac{2\pi}{3L}\right)^{-1} \qquad (24) \\
&\quad \exp i\left[\frac{\pi}{3L}(2x_1 - x_2)(2n_1 - n_2) + \frac{\pi}{L}x_2 n_2\right] \\
&\quad \exp -i\left[\frac{\pi}{3L}(2x_1' - x_2')(2n_1 - n_2) + \frac{\pi}{L}x_2' n_2\right].
\end{aligned}
$$

It has been shown by Mersereau that one can move back and forth between the **x**-basis and the **k**-basis defined above in $\mathcal{O}(N \ln N)$ steps by the forward and backward Hexagonally Discrete Fourier Transforms (HDFT) when $L = 2^m$. We mention in passing that the $\langle \mathbf{x}|d\rangle$'s being real leads to a further saving in computational time over what has been described by Mersereau.

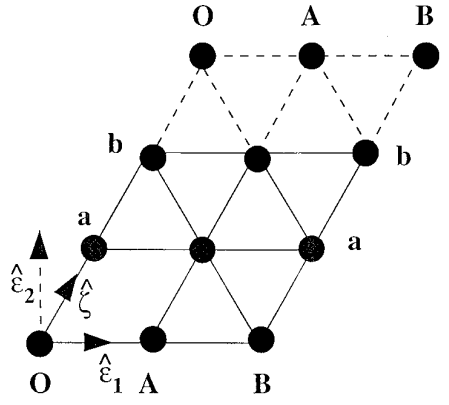

FIG. 4. A triangular lattice periodic in the $\hat{\zeta}$-direction and finite along $\hat{e}_1$ with $L_1 = L_2 = 3$.

4. THE FINITE TRIANGULAR LATTICE

We now show how boundaries can be introduced *without* losing the asymptotically linear nature of our algorithms. The finite array can be driven by currents injected or extracted through the open edges. To keep things as simple as possible, we discuss a lattice which is periodic in the y-direction and open in the x-direction (see Fig. 4). Square arrays with such boundary conditions have been repeatedly used by many authors in numerical studies [38, 39]. We can conveniently study the G_0^{-1} operator for this configuration by separating it into two parts, namely,

$$
G_0^{-1} = P - B, \qquad (25)
$$

where P is the rectangularly periodic operator for the triangular lattice given by Eq. (16) and B is the boundary operator defined by

$$
\begin{aligned}
\langle \mathbf{x}'|B|\mathbf{x}\rangle &= \delta_{x_1,x_0}[2\delta_{\mathbf{x},\mathbf{x}'} - \delta_{x_1-1,x_1'}\delta_{x_2,x_2'} - \delta_{x_1-1,x_1'}\delta_{x_2+1,x_2'}] \\
&\quad + \delta_{x_1,x_0+L_1-1}[2\delta_{\mathbf{x},\mathbf{x}'} - \delta_{x_1+1,x_1'}\delta_{x_2,x_2'} - \delta_{x_1+1,x_1'}\delta_{x_2-1,x_2'}]. \qquad (26)
\end{aligned}
$$

One can easily check that B deletes all the bonds required to introduce boundaries along $x = x_0$ and $x = x_0 + L_1 - 1$.

We examine next the **k** basis defined by

$$
\langle \mathbf{x}|\mathbf{k}\rangle \propto \cos\kappa_1 x_1 \cos\kappa_2(2x_2 + x_1), \qquad (27)
$$

where $\mathbf{k} = k_1\hat{\varepsilon}_1 + k_2\hat{\varepsilon}_2$, and $\kappa_2 = (\sqrt{3}/2)k_2$, $\kappa_1 = (1/2)k_1$, as in Subsection 3.2. However, in this case $\mathbf{x} = x_2\hat{\zeta} + x_1\hat{\varepsilon}_1$ with $\hat{\varepsilon}_i \cdot \hat{\varepsilon}_j = \delta_{ij}$ and $\hat{\zeta} = (\sqrt{3}/2)\hat{\varepsilon}_2 + (1/2)\hat{\varepsilon}_1$.

To motivate this choice, we note that the wavefunctions on the r. h. s. of this equation can be constructed as linear combinations of the degenerate hexagonally periodic wavefunctions listed in Subsection 3.2 and can further be made to satisfy at least in part, the appropriate boundary conditions for our configuration (see below). The **k**-basis is, moreover, accessible from $\{|\mathbf{x}\rangle\}$ through a fast transform.

The normalizations on the eigenfunctions are easily determined to be

$$\langle \mathbf{k}|\mathbf{k}'\rangle = \langle k_1, k_2|k_1', k_2'\rangle = \begin{cases} L_1L_2 & \text{if } \mathbf{k} = \mathbf{k}' = 0 \\ \dfrac{L_1L_2}{2} & \text{if } k_i = k_i' = 0;\ i = 1 \text{ or } 2 \\ \dfrac{L_1L_2}{4} & \text{if } k_i = k_i' \neq 0;\ i = 1, 2. \end{cases} \tag{28}$$

We shall, however, work with the unnormalized eigenfunctions and normalize them at the appropriate junctures.

For these functions to be periodic under $x_2 \to x_2 + L_2$ as required by the geometry of our configuration, we must have $\kappa_2 = (m_2\pi)/L_2$, $m_2 = 0, 1, ..., L_2 - 1$ but can choose x_2 arbitrarily. We shall for convenience work with $x_2 = 0, 1, ..., L_2 - 1$.

As before, we can show that the operator P is diagonal in the **k** basis. Indeed,

$$\begin{aligned} \langle \mathbf{k}|P|\mathbf{k}'\rangle &= \sum_{\mathbf{x}',\mathbf{x}} \langle \mathbf{k}|\mathbf{x}\rangle\langle \mathbf{x}|P|\mathbf{x}'\rangle\langle \mathbf{x}'|\mathbf{k}'\rangle \\ &= \sum_{\mathbf{x}',\mathbf{x}} \langle \mathbf{k}|\mathbf{x}\rangle[6\delta_{\mathbf{x},\mathbf{x}'} - \delta_{x_1\pm1,x_1'}\delta_{x_2,x_2'} \\ &\quad - \delta_{x_1\pm1,x_1'}\delta_{x_2\mp1,x_2'} - \delta_{x_1,x_1'}\delta_{x_2\pm1,x_2'}] \\ &\quad \cos\kappa_1'x_1' \cos\kappa_2'(2x_2' + x_1') \\ &= \sum_{\mathbf{x}} \langle \mathbf{k}|\mathbf{x}\rangle(6 - 4\cos\kappa_1\cos\kappa_2 - 2\cos\kappa_2)\langle \mathbf{x}|\mathbf{k}'\rangle \\ &= \lambda_{\kappa_1,\kappa_2}\langle \mathbf{k}|\mathbf{k}'\rangle = \lambda_{\kappa_1,\kappa_2}\delta_{\mathbf{k},\mathbf{k}'}. \end{aligned} \tag{29}$$

On the other hand, B is only block diagonal, at best. Indeed, $\langle \mathbf{x}|B|\mathbf{k}'\rangle$ can be brought close to being proportional to $\langle \mathbf{x}|\mathbf{k}'\rangle$ but not quite. More specifically, by choosing $x_0 = \frac{1}{2}$ and $\kappa_1' = \pi m_1'/L_1$, $m_1' = 0, 1, ..., L_1 - 1$, we get

$$\langle \mathbf{x}|B|\mathbf{k}'\rangle = 2(1 - \cos\kappa_2')[\delta_{x_1,1/2} + \delta_{x_1,L_1-1/2}]\langle \mathbf{x}|\mathbf{k}'\rangle. \tag{30}$$

From this equation it immediately follows that

$$\begin{aligned} \langle \mathbf{k}|B|\mathbf{k}'\rangle &= \sum_{\mathbf{x}} \langle \mathbf{k}|B|\mathbf{x}\rangle\langle \mathbf{x}|\mathbf{k}'\rangle \\ &= 2(1 - \cos\kappa_2')\frac{L_2}{2}\left[\cos\frac{\kappa_1}{2}\cos\frac{\kappa_1'}{2}\right. \\ &\quad \left. - \cos\frac{\kappa_1(2L_1 - 1)}{2}\cos\frac{\kappa_1'(2L_1 - 1)}{2}\right]\delta_{\kappa_2,\kappa_2'} \\ &= L_2(1 - \cos\kappa_2')[1 + (-1)^{m_1+m_1'}]\cos\frac{m_1\pi}{2L_1} \\ &\quad \cos\frac{m_1'\pi}{2L_1}\delta_{\kappa_2,\kappa_2'}, \end{aligned} \tag{31}$$

where $\kappa_1 = \pi m_1/L_1$ and $\kappa_1' = \pi m_1'/L_1$. We note that for $\kappa_2 = \kappa_2' = 0$, the r. h. s. vanishes. Thus in the $\kappa_2 = 0$ sector, G_0^{-1} is diagonal. Furthermore, we note that if $(m_1 + m_1')$ is odd, the corresponding element of B is zero, signifying that odd and even m_1 values do not mix.

This, in turn, implies that there are two blocks in B corresponding to every non-zero value of κ_2. One of these, of size $[L_1/2]$ (where $[m]$ is the largest integer contained in m) corresponds to odd m_1 and m_1' while the other of size $[(L_1 + 1)/2]$ corresponds to even values of m_1 and m_1'. If we denote these two blocks by $B^{oo}(\kappa_2)$ and $B^{ee}(\kappa_2)$ (for *odd-odd* and *even-even*), respectively, we see that from Eqs. (28) and (31) that their matrix elements, in terms of *normalized* basis vectors, are

$$\begin{aligned} \frac{\langle \kappa_1\kappa_2|B^{oo}|\kappa_1'\kappa_2'\rangle}{\langle \kappa_1\kappa_2|\kappa_1'\kappa_2'\rangle} &= \frac{\langle m_1|B^{oo}(\kappa_2)|m_1'\rangle}{\langle m_1|m_1'\rangle_{\kappa_2}} \\ &= \frac{8}{L_1}(1 - \cos\kappa_2)\cos\frac{m_1\pi}{2L_1}\cos\frac{m_1'\pi}{2L_1} \end{aligned} \tag{32}$$

and

$$\begin{aligned} \frac{\langle m_1'|B^{ee}(\kappa_2)|m_1\rangle}{\langle m_1|m_1'\rangle_{\kappa_2}} &= \frac{8}{L_1}(1 - \cos\kappa_2)\left(1 - \frac{1}{2}\delta_{m_1,0}\right) \\ &\quad \cos\frac{m_1\pi}{2L_1}\cos\frac{m_1'\pi}{2L_1}. \end{aligned} \tag{33}$$

We point out that since $\langle m_1 = 0|B^{ee}(\kappa_2)|m_1\rangle = (1/2)\langle m_1|B^{ee}(\kappa_2)|m_1 = 0\rangle$, $B^{ee}(\kappa_2)$ is not symmetric, while $B^{oo}(\kappa_2)$ clearly is.

It is worth mentioning that the boundary matrix for the finite *square* lattice commutes with the corresponding periodic matrix and hence the two can be simultaneously diagonalized. Even this turns out to be unnecessary, for

that case, because we can make B a null operator, satisfying $B|\mathbf{k}\rangle = 0\ \forall \mathbf{k}$, by choosing $\langle \mathbf{x}|\mathbf{k}\rangle$ as in Eq. (13) and letting the origin lie on the dual lattice.

Returning to $G_0^{-1} = P - B$, we note that this differs from $-B$ only in its diagonal elements. It follows that G_0^{-1} is diagonal in the $\kappa_2 = 0$ sector and each of the blocks in it corresponding to a given $\kappa_2 = n_2\pi/L_2 \neq 0$ can be written as

$$\begin{bmatrix} \lambda_{m_1,m_2} - pAC_{m_1}C_{m_1} & -pAC_{m_1+2}C_{m_1} & \cdots & -pAC_{m_1+q}C_{m_1} \\ -AC_{m_1}C_{m_1+2} & \lambda_{m_1+2,m_2} - AC_{m_1+2}C_{m_1+2} & \cdots & \vdots \\ \vdots & \ddots & \cdots & \vdots \\ -AC_{m_1}C_{m_1+q} & & & \lambda_{m_1+q,m_2} - AC_{m_1+q}C_{m_1+q} \end{bmatrix}, \tag{34}$$

where λ_{m_1,m_2} is given by substituting values of κ_1 and κ_2 in Eq. (29), $p = 1$ (oo case), $p = \frac{1}{2}$ (ee case), $A = 8/L_1(1 - \cos\kappa_2)$, and $C_{m_1} = \cos(m_1\pi)/(2L_1)$. The starting value of m_1 is 1 (oo case) or 0 (ee case) while $m_1 + q = L_1 - 1$ (oo case) or L_1 (ee case).

Having explicitly determined the forms of P and B in the $\mathbf{k}$-basis we can write

$$G_0^{-1} = P - (B^{oo} \oplus B^{ee}) = (G_0^{-1})^{oo} \oplus (G_0^{-1})^{ee}. \tag{35}$$

Each of these blocks can be individually diagonalized to arrive at the eigenvalues and eigenvectors of G_0^{-1}. The eigenbasis of G_0^{-1} can, unfortunately, not be accessed from the position basis through any known fast transform, and we shall, therefore, continue working in the $\mathbf{k}$-basis in preference to carrying out these diagonalizations. This is because much as $G_0(\mathbf{k}, \mathbf{k}')$ is not diagonal, each block in it can be reduced by simple manipulations of the rows to an effectively tridiagonal matrix, which can be solved for $\langle \mathbf{k}|\dot{\theta}\rangle$, in terms of $\langle \mathbf{k}|d\rangle$, in essentially linear order. Since $\langle \mathbf{k}|d\rangle = \sum_{\mathbf{x}} \langle \mathbf{k}|\mathbf{x}\rangle\langle \mathbf{x}|d\rangle$ can be obtained from $\langle \mathbf{x}|d\rangle$ through a fast transform and $\langle \mathbf{x}|\dot{\theta}\rangle = \sum_{\mathbf{k}} \langle \vec{x}|\mathbf{k}\rangle\langle \mathbf{k}|\dot{\theta}\rangle$ from $\langle \mathbf{k}|\dot{\theta}\rangle$ likewise, the entire procedure becomes effectively linear.

Since G^{ee} is diagonal in the $\kappa_2 = 0$ sector, one can solve directly for $d(x_1, x_2)$ instead of using the tridiagonal procedures. Furthermore, in this sector, setting $d(\kappa_1 = 0, \kappa_2 = 0) = 0$ removes the zero mode and automatically fixes the gauge by forcing $\dot{\theta}_i$ to satisfy $\sum_i \dot{\theta}_i = 0$.

To see this in explicit detail we recall that in solving

$$G[u] = [v], \tag{36}$$

where G is of the form given in Eq. (34) for $[u]$ in terms of $[v]$, scalar multiplication and addition are allowed operations on rows but not on columns [40].

Now, from Eq. (34), we see that by multiplying the first row by $C_{m_1+2}/(pC_{m_1})$ and subtracting from it the second, we reduce G to

$$\begin{bmatrix} \lambda_{m_1,m_2}C_{m_1+2}/(pC_{m_1}) & -\lambda_{m_1+2,m_2} & 0 & 0 \\ -AC_{m_1}C_{m_1+2} & \lambda_{m_1+2,m_2} - AC_{m_1+2}C_{m_1+2} & \cdots & \cdots \\ \vdots & \ddots & \cdots & \vdots \\ -AC_{m_1}C_{m_1+q} & & & \lambda_{m_1+q,m_2} - AC_{m_1+q}C_{m_1+q} \end{bmatrix}. \tag{37}$$

By further multiplying the $(r+1)^{\text{st}}$ row by C_{m_1+2r+2}/C_{m_1+2r} and subtracting from it the $(r+2)^{\text{nd}}$ row $r = 1, \ldots, q-2$, we turn G into

$$\begin{bmatrix} \lambda_{m_1,m_2} C_{m_1+2}/(pC_{m_1}) & -\lambda_{m_1+2,m_2} & 0 & 0 \\ 0 & \lambda_{m_1+2,m_2} C_{m_1+4}/C_{m_1+2} & -\lambda_{m_1+4,m_2} & 0 \\ \vdots & \ddots & \cdots & \vdots \\ -AC_{m_1} C_{m_1+q} & & & \lambda_{m_1+q,m_2} - AC_{m_1+q} C_{m_1+q} \end{bmatrix}, \tag{38}$$

i.e., into a matrix which is non-zero only along its diagonal, super-diagonal, and last row. A three-band matrix of this form has (i) the same number of elements as the tridiagonal matrix and (ii) is amenable to a fast $\mathcal{O}(N)$ solution which is similar to that used in tridiagonal systems. We remark that for a given configuration the numbers $C_{m_1+2r+2}/(pC_{m_1+2r})$ are constants and need be determined once at the outset.

We conclude this section by verifying that for a lattice which is rectangularly periodic in the y-direction, the direct and the inverse transforms are both separable with respect to the arguments concerned. More explicitly,

$$\begin{aligned} \langle \mathbf{k}|\mathbf{d}\rangle &= \sum_{\mathbf{n}} \langle \mathbf{k}|\mathbf{x}\rangle\langle \mathbf{x}|\mathbf{d}\rangle \\ &= \sum_{\mathbf{x}} d(x_1, x_2) \cos\frac{m_1\pi x_1}{L_1} \cos\frac{m_2\pi(2x_2 + x_1)}{L_2} \\ &= \sum_{x_1} \cos\frac{m_1\pi x_1}{L_1} \sum_{x_2} d(x_1, x_2) \left[\cos\frac{2m_2\pi x_2}{L_2} \cos\frac{m_2\pi x_1}{L_2} \right. \\ &\quad \left. - \sin\frac{2m_2\pi x_2}{L_2} \sin\frac{m_2\pi x_1}{L_2} \right], \end{aligned} \tag{39}$$

where $x_2 = 0, 1, \ldots, L_2 - 1$ and $x_1 = \frac{1}{2}, \frac{3}{2}, \ldots, L_1 - \frac{1}{2}$. The summation over x_2 can be performed by noting that $\sum_{x_1} d(x_1, x_2) \cos(2m_2\pi x_2/L_2)$ and $\sum_{x_1} d(x_1, x_2) \sin(2m_2\pi x_2/L_2)$ are the real and imaginary parts of the fourier transform of $d(x_1, x_2)$. This (fast) fourier transform is followed by the multiplication of the real (imaginary) parts by $\cos(m_2\pi x_1/L_2)$ ($-\sin(m_2\pi x_1/L_2)$ and the addition of the resulting products, to get the function multiplying $\cos(m_1\pi x_1/L_1)$ in Eq. (39). Finally, the sum over x_1 can be performed by using the fast cosine transform. The complexity of the whole procedure is then essentially $\mathcal{O}(N \ln N)$. The backward transform, i.e.,

$$\begin{aligned} \langle \mathbf{x}|\theta\rangle &= \sum_{\mathbf{k}} \langle \mathbf{x}|\mathbf{k}\rangle\langle \mathbf{k}|d'\rangle \\ &= \sum_{m_1,m_2} d'(\kappa_1, \kappa_2) \cos\frac{m_1\pi x_1}{L_1} \cos\frac{m_2\pi(2x_2 + x_1)}{L_2} \end{aligned}$$

can likewise be performed with a complexity $\mathcal{O}(N \ln N)$. By contrast, for a lattice with *hexagonal* periodicity in the y-direction, W and $\tilde{W}$ are *not* separable in x_1 and x_2. They can nevertheless be performed with a complexity $\mathcal{O}(N \ln N)$ using the HDFT procedures outlined in [36].

5. SUMMARY AND DISCUSSION

To summarize, we have extended to triangular arrays the fast algorithms, which were so far available only for square geometries. More specifically, we have developed algorithms for periodic triangular lattices and those with one set of parallel edges free. In treating the former, we have kept track of the fact that a triangular lattice admits rectangular as well as hexagonal periodicity and have shown that the rectangularly periodic case is a relatively straightforward extension of the square case. On the other hand, the hexagonally periodic situation is quite distinct in that the eigenfunctions of the corresponding discrete laplacian are not separable in x_1 and x_2. Their eigenbasis can nevertheless be accessed from the position basis in $\mathcal{O}(N \ln N)$ steps by the Hexagonally Discrete Fourier Transforms. This circumstance has allowed us to take the algorithm through. The finite case is rather more difficult for the triangular lattice than it is for the square. This is because the creation of a boundary in the former requires the removal of two bonds placed obliquely with respect to each other, rather than one. This case therefore requires a new approach and this has been developed in the paper. In particular we have broken up the inverse laplacian G_0^{-1} into a periodic (P) and a boundary (B) matrix and have shown that for a specific choice of the basis both B and $P - B = G_0^{-1}$ take on forms which are amenable to diagonalization in linear order. This has allowed us to present for the finite case an algorithm which is asymptotically linear to within constants and factors of $\ln N$.

We should also mention that we have not fully exploited the symmetries of the triangular lattice in this paper. In particular, we still need to investigate the circumstances under which the wavefunctions related by symmetry transformations to the one we have actually used (see Eq. (22)) are more convenient.

It is also interesting to note that the approach adopted in this paper has much in common with the one used in Ref. [32] to treat missing bond defects in square arrays. There, too G^{-1} was decomposed into two parts: one (G_0^{-1}) for the perfect finite lattice and the other (h) for the defect, $G^{-1} = G_0^{-1} - h$, with $G_0^{-1} = P - B$ and $[P, B] = 0$. For a linear defect with n ($<N_i$) broken bonds $[G_0^{-1}, h] \neq 0$. The form of h, however, makes the problem amenable to a perturbative approach rather than to the tridiagonalization described in this paper.

It is also interesting to note that the case discussed in Section 4 has a close resemblance to the FACR method [40]. Indeed both the approaches combine a fast transform with a tridiagonalization routine. It should however be pointed out that for the finite triangular array, the fast transform involves both variables. Furthermore, the $G_0(\mathbf{k}, \mathbf{k}')$ of Eq. (34) becomes tridiagonal only after considerable manipulations.

Finally we observe that for a hexagonally periodic lattice, equivalent points in different tiles (see Ref. [36]) can be exchanged to create a new fundamental period. These periods therefore come in several shapes of which Fig. 1 is but one example. The corresponding eigenvalues and eigenfunctions, however, remain unaltered and the $\mathcal{O}(N \ln N)$ algorithm continues to be equally applicable to each of them. These shapes can serve as starting points for creating several different finite lattices. The various types of boundaries which result are especially significant in view of the interesting question: For which class of boundaries does the matrix B commute with P? Indeed if there are cases for which $[P, B] = 0$, they will automatically lead to $\mathcal{O}(N \ln N)$ algorithms.

ACKNOWLEDGMENTS

The authors thank Jitendra Das for pointing out Ref. [36] and Shreesh Jadhav for help with programming.

REFERENCES

1. J. E. Mooij and G. B. J. Schon (Eds.), Proceedings of the NATO advanced research workshop on coherence in superconducting networks, *Physica B* **152,** 1 (1988).
2. H. S. J. van der Zant, F. C. Fritschy, T. P. Orlando, and J. E. Mooij, *Phys. Rev. Lett.* **66,** 2531 (1991).
3. P. Minnhagen, *Rev. Mod. Phys.* **59,** 1001 (1987).
4. P. Martinoli, *Helv. Phys. Acta* **80,** 128 (1987); P. Martinoli, *Physica B* **152,** 146 (1988); Ch. Leemann, Ph. Lerch, G. A. Racine, and P. Martinoli, *Phys. Rev. Lett.* **56,** 1291 (1986).
5. K. K. Mon and S. Teitel, *Phys. Rev. Lett.* **62,** 673 (1989).
6. S. Teitel and C. Jayaprakash, *Phys. Rev. Lett.* **51,** 1999 (1983).
7. W. Xia and P. L. Leath, *Phys. Rev. Lett.* **63,** 1428 (1991).
8. D. Dominguez, J. V. Jose, A. Karma, and C. Weicko, *Phys. Rev. Lett.* **67,** 2367 (1991).
9. C. J. Lobb, D. W. Abraham, and M. Tinkham, *Phys. Rev. B* **27,** 150 (1983).
10. R. Theron, J. B. Sigmond, Ch. Lemann, H. Beck, P. Matinoli, and P. Minnhagen, *Phys. Rev. Lett.* **71,** 1246 (1993).
11. S. E. Korshunov, *Physica B* **152,** 261 (1988).
12. A. Larkin, Y. Ovchinikov, and A. Schmid, *Physica B* **152,** 266 (1988).
13. U. Eckern and A. Schmid, *Phys. Rev. B* **39,** 6441 (1989).
14. U. Eckern and E. B. Sonin, *Phys. Rev. B* **47,** 505 (1993).
15. H. S. J. van der Zant, F. C. Fritschy, T. P. Orlando, and J. E. Mooij, *Europhys. Lett.* **18,** 343 (1992).
16. P. A. Bobbert, *Phys. Rev. B* **45,** 7540 (1992).
17. U. Geigenmuller, C. J. Lobb, and C. B. Whan, *Phys. Rev. B* **47,** 348 (1993).
18. Wenbin Yu and D. Stroud, *Phys. Rev. B* **49,** 6174 (1994).
19. T. J. Hagenaars, P. H. E. Tiesinga, J. E. van Himbergen, and J. V. Jose, *Phys. Rev. B* **50,** 1143 (1994).
20. R. Mehrotra, S. Datta, and D. Sahdev, *Mod. Phys. Lett. B* to appear.
21. W. J. Elion, J. J. Wachters, L. L. Sohn, and J. E. Mooij, *Phys. Rev. Lett.* **71,** 2311 (1993).
22. R. Theron, S. E. Korshunov, J. B. Sigmond, Ch. Lemann, and P. Matinoli, *Phys. Rev. Lett.* **71,** 1246 (1993).
23. S. E. Korshunov, A. Vallat, and H. Beck, *Phys. Rev. B* **51,** 3071 (1995).
24. W. Y. Shih and D. Stroud, *Phys. Rev. B* **30,** 6774 (1984).
25. M. Y. Choi and S. Doniach, *Phys. Rev. B* **31,** 4516 (1985).
26. L. L. Sohn, M. S. Rzchowski, J. U. Free, M. Tinkham, and C. J. Lobb, *Phys. Rev. B* **45,** 3003 (1991).
27. P. N. Strenski and S. Doniach, *J. Appl. Phys.* **57,** 867 (1985).
28. S. Das, S. Datta, M. Dutta, S. Jain, and D. Sahdev, *Physica D* **91,** 278 (1996); S. Das, S. Datta, M. K. Verma, D. Sahdev, and R. Mehrotra, *Physica D* **91,** 292 (1996).
29. S. R. Shenoy, *J. Phys. C* **18,** 5163 (1985); **20,** 2479(E) (1987).
30. V. Ambegaokar and B. I. Halperin, *Phys. Rev. Lett.* **22,** 1364 (1969); Errata, **23,** 274 (1969).
31. H. Eikmans and J. E. van Himbergen, *Phys. Rev. B* **41,** 8927 (1990).
32. S. Datta, S. Das, D. Sahdev, R. Mehrotra, and S. R. Shenoy, *Phys. Rev. B* **54,** 3545 (1996).
33. Dominguez *et al., Phys. Rev. Lett.* **75,** 4670 (1995).
34. P. A. M. Dirac, *The Principles of Quantum Mechanics* (Oxford Univ. Press, London, 1958).
35. J. J. Sakurai, *Modern Quantum Mechanics* (Benjamin–Cummings, Redwood City, CA, 1985).
36. R. M. Merserau, *Proc. IEEE* **67,** 930 (1979).
37. J. D. Jackson, *Classical Electrodynamics* (Wiley, New York, 1962).
38. P. L. Leath and W. Xia, *Phys. Rev. B* **44,** 9619 (1991).
39. D. Dominguez, *Phys. Rev. Lett.* **72,** 3096 (1994).
40. W. H. Press, S. A. Teukolksy, W. T. Vetterling, and B. P. Plannery, *Numerical Recipes* (Cambridge Univ. Press, Cambridge, 1986).